



Green, T.A. and Roy, S. (2017) Application of a duplex diffusion layer model to pulse reverse plating. Transactions of the Institute of Metal Finishing, 95 (1). pp. 46-51. ISSN 0020-2967 , <http://dx.doi.org/10.1080/00202967.2016.1214354>

This version is available at <https://strathprints.strath.ac.uk/56747/>

Strathprints is designed to allow users to access the research output of the University of Strathclyde. Unless otherwise explicitly stated on the manuscript, Copyright © and Moral Rights for the papers on this site are retained by the individual authors and/or other copyright owners. Please check the manuscript for details of any other licences that may have been applied. You may not engage in further distribution of the material for any profitmaking activities or any commercial gain. You may freely distribute both the url (<https://strathprints.strath.ac.uk/>) and the content of this paper for research or private study, educational, or not-for-profit purposes without prior permission or charge.

Any correspondence concerning this service should be sent to the Strathprints administrator: strathprints@strath.ac.uk

7th European Pulse Plating Seminar – submission to *Transactions of the IMF*

Application of a Duplex Diffusion Layer Model to Pulse Reverse Plating

T.A. Green* and S. Roy

Department of Chemical and Process Engineering

University of Strathclyde,

Glasgow, G1 1XJ

* Corresponding Author, email: todd.green@strath.ac.uk

Keywords: electrodeposition, pulse plating, diffusion layer, mass transfer

Abstract

The application of Ibl's duplex diffusion layer model to the analysis of mass transport in pulse reverse plating with bipolar current pulses has been investigated. Although originally proposed to describe normal pulse plating, Yin has recently extended Ibl's model to include pulse reverse plating. Using the expressions derived by Yin the pulse limiting current density was determined over a wide range of pulse plating conditions, and then compared to values calculated using more accurate numerical solutions. In general, there was good agreement between the two approaches which demonstrated the essential validity of Yin's extension to Ibl's original model. The simplified model is most accurate at long duty cycles, small dimensionless pulse times and for low values of the dimensionless pulse reverse current where its underlying assumptions are most likely to be valid. At very long dimensionless pulse times (i.e. $T^* > 1$) the model becomes increasingly inaccurate and its use in these circumstances cannot be justified.

List of Symbols

C	concentration
C_b	bulk concentration
C_s	surface concentration
D	diffusion coefficient
F	Faraday constant
i	current density
i_{LIM}	steady-state limiting current density
i_p	peak forward (cathodic) current density
i_p^l	peak reverse (anodic) current density
i_{pLIM}	pulse limiting current density
i_{pLIM}^*	dimensionless pulse limiting current density
i_{rpLIM}^*	dimensionless pulse reverse limiting current density
i_p^{l*}	dimensionless peak reverse current density
m	summation index
n	number of electrons transferred in reaction
t_{on}	pulse on time
t_{off}	pulse off time
t_{rev}	pulse reverse time
T	pulse time
T^*	dimensionless pulse time
α	constant
δ	thickness of steady-state diffusion layer
δ_p	thickness of pulsing diffusion layer
λ_m	dimensionless summation parameter
θ	duty cycle

1 Introduction

Pulse plating has been used extensively in the surface finishing industries to deposit a wide range of materials including metals, alloys, composite materials and semiconductors.¹⁻⁵ By careful choice of the pulse parameters it is possible to influence the mass transport, kinetics and electro-crystallisation aspects of the deposition process and thereby obtain materials with enhanced characteristics. Theoretical and experimental aspects of pulse plating were reviewed in 1986 in a book edited by Puipe and Leaman¹ and this has been recently updated by a monograph by Hansal and Roy² in 2012. Additionally, a number of useful review articles on the subject of pulse plating are also available.³⁻⁵

A critical issue in DC or pulse plating is evaluating the mass transport of reacting species to the electrode surface as this determines the maximum rate at which plating can occur⁶ and can also influence the current distribution.⁷ For DC plating, a simple steady-state model can be used where it is assumed that mass transport occurs only by diffusion close to the electrode surface, while convection dominates further away. This results in the formation of a well characterised stagnant (Brunner-Nernst) diffusion layer near the electrode surface whose thickness, δ , determines the attainable limiting current, i_{LIM} . Similar constraints also apply in pulse plating but the identification of mass transport limitations under transient (i.e. non steady-state) conditions is both conceptually and computationally more difficult to assess.

A simple means for describing mass transport in pulse plating is the dual diffusion layer model originally proposed by Ibl in 1980.⁸ Although this model is based on numerous simplifications and approximations, it gives a good qualitative and quantitative understanding of mass transport limitations in pulse plating systems. Ibl's model was originally developed for the case of pulse plating with simple rectangular unipolar current pulses. It has been tested theoretically against more precise mass transport models and typically shows agreement within 10%.⁸ Additional refinements proposed by Datta and Landolt⁹ have further improved the accuracy of the original model.

Despite the existence of more accurate numerical models of mass transport during pulse plating, Ibl's duplex double layer model layer has some important advantages. Firstly, it allows one to easily visualise the transport processes occurring at the electrode surface, while providing a plausible insight into the phenomena involved.⁸ Secondly, it is more computationally simple to use than the numerical solutions proposed by others. For these reasons it is still common¹⁰⁻¹² to model mass transport in pulse plating experiments in terms of Ibl's model.

The original model was developed for conventional pulse plating but in 1996 Yin¹³ proposed an extended model for the case of pulse plating using bipolar rectangular current pulses. This was a useful development as pulse reverse plating has become an increasingly important technique, especially in the manufacture of printed circuit boards.^{2,14} It is also routinely applied when improvements in the material distribution (i.e. throwing power) are required.^{14,15} Despite such motivations there has been no attempt to test Yin's model either experimentally or theoretically. The aim of the present communication is to undertake such an evaluation and thereby verify that Ibl's model can be used to determine mass transport effects under pulse reverse plating conditions.

2 Background

Before discussing the various mass transport models in detail, it is necessary to define the relevant pulse parameters for both normal pulse plating with rectangular unipolar pulses (Fig. 1a) and that for pulse reverse plating with bipolar rectangular pulses (Fig. 1b). In the former case we can define an on-time with a peak cathodic current of $i = i_p$ and duration t_{on} followed by an off-time with a duration of t_{off} and where $i = 0$. The total pulse time, T , is given by $T = t_{on} + t_{off}$ and the duty cycle as $\theta = t_{on}/T$. For pulse reverse plating we can define a peak cathodic current, i_p , of duration t_{on} followed by a reverse (anodic) current of i'_p and duration t_{rev} . The pulse time is then $T = t_{on} + t_{rev}$ and the cathodic duty cycle is $\theta = t_{on}/T$. It should be noted that all theoretical treatments of mass-transport effects in pulse plating assume perfect rectangular

pulses, but in reality this may not be fully realised due to double layer charging/discharging effects or limitations of the pulse rectifier.^{1,2}

As noted in the introduction, in 1980 Ibl⁸ presented a mass transport model applicable to deposition using simple rectangular unipolar current pulses. He introduced the concept of a dual diffusion layer consisting of an inner pulsating diffusion layer of thickness δ_p coupled to an outer static diffusion layer (Figure 2). The outer concentration profile corresponds to the normal Nernst diffusion layer, with a corresponding steady state limiting current of i_{LIM} . The inner concentration profile is associated with a pulse limiting current, i_{pLIM} , which is the current density at which the surface concentration reaches zero at the end of the pulse (Figure 2). According to Ibl's model these quantities can be expressed by the following equations:

$$i_{pLIM} = i_{LIM} \left[\frac{\delta_p}{\delta} (1 - \theta) + \theta \right]^{-1} \quad (1)$$

with

$$\delta_p = [2Dt_{on}(1 - \theta)]^{1/2} \quad (2)$$

Crucially, while δ is controlled by the hydrodynamic conditions, δ_p depends only on the pulse parameters t_{on} and θ and the diffusion coefficient, D , of the reacting species. Experimentally it is found that if either the steady-state, i_{LIM} , or pulse limiting, i_{pLIM} , are exceeded this results in a reduced current efficiency and the formation of rough or dendritic deposits.^{10,16} Therefore it is necessary to choose pulse parameters carefully in order to not exceed transient or steady-state mass transport conditions.^{6,17}

An important question regarding these simplified models is whether they accurately describe the mass transport conditions under pulse plating conditions. In the case of rectangular current pulses it is possible to obtain numerical solutions without resorting to the approximations employed by Ibl. For example, both Cheh^{18,19} and Chin^{20,21} have derived more accurate solutions for unipolar and bipolar pulse plating and have also verified these results experimentally by comparing them with pulse limiting currents derived from transition time

measurements. Ibl⁸ initially found reasonable agreement between his and Cheh's solution but Datta and Landolt⁹ subsequently found that this could be improved using the following revised expression for δ_p :

$$\delta_p = \left[\frac{4}{\pi} D t_{on} (1 - \theta) \right]^{1/2} \quad (3)$$

Using this modified equation, Datta and Landolt⁹ and later Chin and co-workers²² found that the agreement between the Ibl model and the more accurate expressions was typically 5 - 10% over a wide range of pulse parameters, lending credibility to the dual diffusion layer concept.

In his 1996 paper Yin¹³ used a similar approach to Ibl⁸ to derive an expression for the pulse limiting current under pulse reverse conditions:

$$i_{rpLIM} = \frac{\frac{nFDC}{\delta_p} + i'_p(1 - \theta) \left(\frac{\delta}{\delta_p} \right)}{1 + \theta \left(\frac{\delta}{\delta_p} - 1 \right)} \quad (4)$$

where n is the number of electrons transferred, F is the Faraday constant and C is the bulk concentration of the reacting species. Note that by setting $i'_p = 0$ equation 4 reduces to equation 1 describing the unipolar case. In a 2008 publication Chang²³ extended this treatment to the case of pulse reverse plating with a relaxation (i.e. zero current) period between the cathodic and anodic pulses. Despite these two studies, there has been no attempt to test these pulse reverse models either experimentally or against numerical solutions and the applicability of Ibl's model to the pulse reverse case is not known. Fortunately, Cheh¹⁹, Chin^{20,21} and Roy²⁴ have provided accurate numerical solutions for the pulse reverse situations so that a means of evaluating the correctness of Yin's proposal is available.

3 Results and Discussion

The main purpose of this paper is to evaluate the applicability of the duplex diffusion model to the case of pulse reverse plating by comparing Yin's approximate expression for the pulse reverse limiting current, i_{rpLIM} , to that calculated from the more accurate numerical solution. In

the latter case we use an expression derived by Roy²⁴ for the dimensionless pulse reverse limiting current, i_{rpLIM}^* :

$$i_{rpLIM}^* = \frac{i_{rpLIM}}{i_{LIM}} = \frac{1 + 2i^* T^* \sum_{m=1}^{\infty} \frac{\exp(\lambda_m(1-\theta)) - 1}{\lambda_m [\exp(\lambda_m) - 1]}}{1 - 2T^* \sum_{m=1}^{\infty} \frac{\exp(\lambda_m(1-\theta)) - 1}{\lambda_m [\exp(\lambda_m) - 1]}} \quad (5)$$

where $\lambda_m = \pi^2(m - 0.5)^2$, m is a summation index, $T^* = DT/\delta^2$ is the dimensionless pulse time and $i^* = i_p/i_{LIM}$ is the dimensionless pulse reverse current. As previously demonstrated by Roy²⁴ this equation is equivalent to those derived by Cheh^{18,19} and Chin.^{20,21} For the unipolar case the equation can be used with $i^* = 0$. Note that a positive sign convention is used for both the anodic and cathodic current in equations 4 and 5. In practice, the calculation of the pulse limiting current does not require the large (or infinite) series summation suggested by equation 5. Typically, convergence is obtained for $m < 10$ but for small dimensionless times (e.g. $T^* < 0.01$) a summation to $m = 100$ or higher was necessary. Equation 1 can also be conveniently rewritten in dimensionless form as:

$$i_{pLIM}^* = \frac{i_{pLIM}}{i_{LIM}} = \frac{1}{\alpha(1-\theta)^{1.5}(\theta T^*)^{0.5} + \theta} \quad (6)$$

The value of the coefficient α is $\sqrt{2}$ for Ibl's original model and $\sqrt{4/\pi}$ for the revised equation.

In order to test the accuracy of the various mass transport models it is necessary to compare equations 4, 5 and 6 under a wide range of pulse conditions. For convenience it is useful to analyse these as plots of dimensionless pulse limiting current (i.e. i_{rpLIM}^* and i_{pLIM}^*) against the dimensionless pulse time, $T^* = DT/\delta^2$. Pulse limiting currents were computed for T^* ranging from 0.001 to 10. For a typical liquid phase diffusion coefficient of $5.0 \times 10^{-6} \text{ cm}^2 \text{ s}^{-1}$ and a diffusion layer thickness of $\delta = 50 \text{ } \mu\text{m}$ this corresponds to pulse times of $T = 5 \text{ ms} - 50 \text{ s}$. The range of duty cycles ($0.01 < \theta < 0.50$) and dimensionless reverse currents ($0 < i^* < 5$)

examined were based on an earlier analysis by Roy²⁴ who determined the practical range of parameters during pulse reverse plating.

Before investigating the pulse reverse model it is instructive to re-examine the simple unipolar case. Figure 3 shows the dimensionless limiting pulse current as a function of duty cycle calculated using equations 5 and 6. Equation 5 predicts values which are within 1% of the values calculated by Chin²⁰⁻²² and also shows the correct limiting behaviour for extremely short pulses $i^*_{pLIM}(T^* \rightarrow 0) = 1/\theta$ and $i^*_{pLIM}(T^* \rightarrow \infty) = 1$ corresponding to infinitely large pulses (i.e. DC plating conditions). Also shown as dotted lines are the pulse limiting currents calculated using equation 6 with two different values of α . Once again, these results are essentially identical to those obtained by Landolt⁹ and Chin.²² Collectively they predict values of i^*_{pLIM} that are generally lower than for the more accurate numerical solution but the agreement is better as the duty cycle increases ($\theta \rightarrow 0.50$). They also show larger deviations for long dimensionless pulse times. Note that while equation 6 correctly predicts $i^*_{pLIM}(T^* \rightarrow 0) = 1/\theta$ it incorrectly predicts $i^*_{pLIM}(T^* \rightarrow \infty) = 0$ and indeed the calculations often show that i^*_{pLIM} is less than unity for $T^* > 1$.

In summarising the unipolar results, we can say that Ibl's original models agrees with the more accurate models to within 1 - 20% over the range $0.01 < T^* < 1$ and $0.01 < \theta < 0.50$ with a mean error of 6%. In contrast, the revised model shows a much improved fit over the same parameter range with typical variations of 1 - 10% and a mean error 3%. These findings are in agreement with earlier studies^{9,22} and indicate that the revised model should always be used when the highest accuracy is desired.

The results for the bipolar case are shown in Figures 4 and 5 and are summarised in Tables 1 and 2. Figure 4 indicates the variation in the dimensionless pulse reverse limiting current as a function of the T^* and i'^* at a fixed duty cycle of $\theta = 0.50$. The solid lines indicate equation 5

while the dotted lines indicate the use of Yin's equation using the two definitions of δ_p . Once again the results obtained using equation 5 agree closely with those given by Chin for pulse reverse plating.^{20,21} The lowest curve represents the unipolar case ($i'^* = 0$) and it can be seen that, at constant T^* , higher values of the pulse reverse limiting current are obtained as i'^* increases. This is expected as larger anodic current pulses will increase the concentration of the reacting ions at the surface (see Figure 2b). Therefore, in the subsequent cathodic pulse a larger current density will be required to reduce the surface concentration to zero at the end of the pulse.^{13,20} Figure 4 also indicates that Yin's equation provides a reasonably good agreement with the more accurate solution over a wide range of T^* values. As was found for the unipolar case, the agreement is worse for $T^* > 1$ and in some cases gave rise to unphysical results (e.g. $i_{pLIM} < 1$ or $i_{pLIM} < 0$).

Figure 5 shows the variation in the dimensionless pulse reverse limiting current as a function of T^* at various values of θ and for $i'^* = 2$. The solid lines show the prediction of equation 5 and the dotted lines those calculated from Yin's equation using the two definitions of δ_p . These results are again essentially identical to those reported by Chin.^{20,21} It can also be seen that the approximate model agrees very well with the numerical solution. As was the case for unipolar pulses, the agreement is worse for low duty cycles and for large dimensionless pulse times, and the revised model is again more accurate than Ibl's model under all conditions.

An additional constraint on pulse reverse plating is the condition that the charge associated with the cathodic pulse must be larger than that associated with the anodic pulse if deposition is to be observed.^{20,24} This is reflected in the black dotted line in Figure 5 which defines the boundary between net deposition and dissolution. Notably, for $\theta < 0.50$ the region of practical deposition always occurs at $T^* < 1$ and this is also the region where the duplex model shows the smallest deviations from the more accurate solutions.

The overall conclusions for the bipolar case are similar to those for the unipolar cases, in that the dual diffusion layer model employing Yin's equation is capable of predicting the pulse limiting current over a wide range of pulse conditions. For the original definition of δ_p and the parameter space $0.001 < T^* < 1$, $0.01 < \theta < 0.50$ and $0 < i'^* < 5$ the variation against the more accurate solution is 1 - 30% with a mean error of 12%. For the corresponding revised definition of δ_p the range is 1 - 10% with a mean error of 4%. The latter result can be compared to a mean error of 3% in the unipolar case over a similar range of pulse conditions.

The main limitation of the simplified Ibl model in pulse and pulse reverse plating is undoubtedly the inaccurate predictions of mass transfer characteristics for long pulse durations (i.e. $T^* > 1$). This is not entirely unexpected as the distinction between the pulsing and stationary diffusion layers becomes less reasonable at long times where essentially steady-state conditions prevail. Generally this is not an issue as pulse times are usually of the order of 0.01 - 1 s, but in some implementations of pulse reverse plating very long (i.e. 1 - 10 s) pulse cycles are employed.^{14,15} In these cases it would be more prudent to use Roy's or Chin's equation to calculate the pulse limiting current.

4 Conclusions

The application of Ibl's duplex diffusion layer model to the modelling of mass transport effects in pulse reverse plating has been investigated. Specifically, we have tested the accuracy of the equations derived by Yin for the pulse reverse limiting current density against the more accurate numerical solution provided by Chin²⁰⁻²² and Roy.²⁴ It was found that the revised model could accurately predict the pulse reverse limiting current density over a wide range of pulse conditions. Deviations from the numerical solutions were of similar magnitude to those calculated for normal pulse plating, and were typically less than 10%. Additionally, the use of the revised definition of δ_p substantially improved the agreement between Ibl and Yin's simple model and the more accurate models. In general the model is most accurate at long duty cycles

($\theta \rightarrow 0.5$), small dimensionless times ($T^* < 1$) and for low values of the dimensionless pulse reverse current ($i^{r*} < 2$). For longer pulse times the model becomes increasingly inaccurate and its use in these circumstances cannot be justified.

References

1. J. C. Puipe, F. Leaman: 'Theory and Practice of Pulse Plating', 1980, Orlando, FL, AESF.
2. W. E. G. Hansal, S. Roy: 'Pulse Plating', 2012, Bad Saulgau, Eugen G. Leuze.
3. A. M. Pesco, H. Y. Cheh: 'Theory and Applications of Periodic Electrolysis', in 'Modern Aspects of Electrochemistry' Vol. 9, (eds. B. E. Conway, J. O'M. Bockris, R. E. White), 251-293; 1989, New York, Plenum Press.
4. D. Landolt, A. Marlot: 'Microstructure and composition of pulse-plated metals and alloys', *Surf. Coat. Technol.*, 2003, **169-170**, 8-13.
5. R. T. C. Choo, A. Toguri, A. M. El-Sherik, U. Erb: 'Mass transfer and electrocrystallization analyses of nanocrystalline nickel production by pulse plating', *J. Appl. Electrochem.*, 1995, **25**, 384-403.
6. S. Roy: 'Mass transfer during pulse deposition', in 'Pulse Plating' (eds. W. E. G. Hansal and S. Roy), 100-122, 2012, Bad Saulgau, Eugen G. Leuze.
7. W. E. G. Hansal, L. Linauer: 'Current distribution', in 'Pulse Plating' (eds. W. E. G. Hansal and S. Roy), 83-99, 2012, Bad Saulgau, Eugen G. Leuze.
8. N. Ibl: 'Some theoretical aspects of pulse electrolysis', *Surf. Technol.*, 1980, **10**, 81-104.
9. M. Datta, D. Landolt: 'Experimental investigation of mass transport in pulse plating', *Surf. Technol.*, 1985, **25**, 97-110.
10. O. Chene, D. Landolt: 'The influence of mass transport on the deposit morphology and the current efficiency in pulse plating of copper', *J. Appl. Electrochem.*, 1989, **29**, 188-194.
11. C. K. Lai, Y. Y. Wang, C. C. Wan: 'Palladium electrodeposition from ammonia-free electrolyte', *J. Electroanal. Chem.*, 1992, **322**, 267-278.
12. N. Tantavichet, M. D. Pritzker: 'Effect of plating mode, thiourea and chloride on the morphology of copper deposits produced in acidic sulphate solutions', *Electrochim. Acta*, 2005, **50**, 1849-1861.
13. K. M. Yin: 'Duplex diffusion layer model for pulse with reverse plating', *Surf. Coat. Technol.*, 1996, **88**, 162-164.

14. P. Leisner, C. Zanella, I. Belov, C. Edstrom, H. Wang: 'Influence of anodic pulses and periodic current reversion on electrodeposits', *Trans. IMF*, 2014, **92**, 336-341.
15. S. Hansal, L. Linauer, W. E. G. Hansal: 'Comparison of simulated pulse plating processes to practical experiments', *Trans. IMF*, 2009, **87**, 102-108.
16. S. Roy: 'Formation of dual diffusion layer by pulsing currents', *Ind. Eng. Chem. Res.*, 2012, **51**, 1756-1760.
17. S. Roy: 'Mass transfer considerations during pulse plating', *Trans. IMF*, 2008, **86**, 87-91
18. H. Y. Cheh: 'Electrodeposition of gold by pulsed current', *J. Electrochem. Soc.*, 1971, **118**, 551-557.
19. H. Y. Cheh: 'The limiting current of deposition by P-R plating', *J. Electrochem. Soc.*, 1971, **118**, 1132-1134.
20. D. T. Chin: 'Mass transfer and current-potential relation in pulse electrolysis', *J. Electrochem. Soc.*, 1983, **130**, 1657-1667
21. J. Y. Wang, D. Balamurugan, D. T. Chin: 'An experimental study of mass transfer in pulse reversal plating', *J. Appl. Electrochem.*, 1992, **22**, 240-246.
22. D. T. Chin, J. Y. Wang, O. Dossenbach, J. M. Locarnini, A. Numanoglu: 'Mass transfer in pulse plating: An experimental study with rectangular cathodic current pulses', *Electrochim. Acta*, 1991, **36**, 625-629.
23. L. M. Chang: 'Diffusion layer model for pulse reverse plating', *J. Alloy Compounds*, 2008, **466**, L19-L22.
24. S. Roy, D. Landolt: 'Determination of the practical range of parameters during reverse-pulse current plating', *J. Appl. Electrochem.*, 1997, **27**, 299-307

		Dimensionless limiting pulse reverse current density, i^*_{rpLIM}		
θ	T^*	Numerical solution (equation 5)	Approximate solution (equation 3 & 4)	Approximate solution (equation 2 & 4)
0.10	0.001	25.63	25.36	24.77
	0.01	21.61	20.99	19.71
	0.1	14.16	13.28	11.59
	1.0	6.038	5.414	4.226
	10	1.221	0.821	0.295
0.50	0.001	3.887	3.895	3.869
	0.01	3.657	3.680	3.604
	0.1	3.034	3.092	2.904
	1.0	1.671	1.836	1.515
	10	1.000	0.155	-0.146

Table 1: Comparison of the dimensionless pulse reverse limiting current density calculated from various models and with $i'^*_{LIM} = 2$.

		Dimensionless limiting pulse reverse current density, i^*_{rpLIM} ,		
i^{**}	T^*	Numerical solution (equation 5)	Approximate solution (equation 3 & 4)	Approximate solution (equation 2 & 4)
0 (unipolar)	0.001	1.962	1.965	1.956
	0.01	1.885	1.893	1.868
	0.1	1.678	1.697	1.635
	1.0	1.224	1.279	1.172
	10	1.000	0.718	0.618
2	0.001	3.887	3.895	3.869
	0.01	3.657	3.680	3.604
	0.1	3.034	3.092	2.904
	1.0	1.671	1.836	1.515
	10	1.000	0.155	-0.146

Table 2: Comparison of the dimensionless pulse reverse limiting current density calculated from various models at a fixed duty cycle of $\theta = 0.5$.

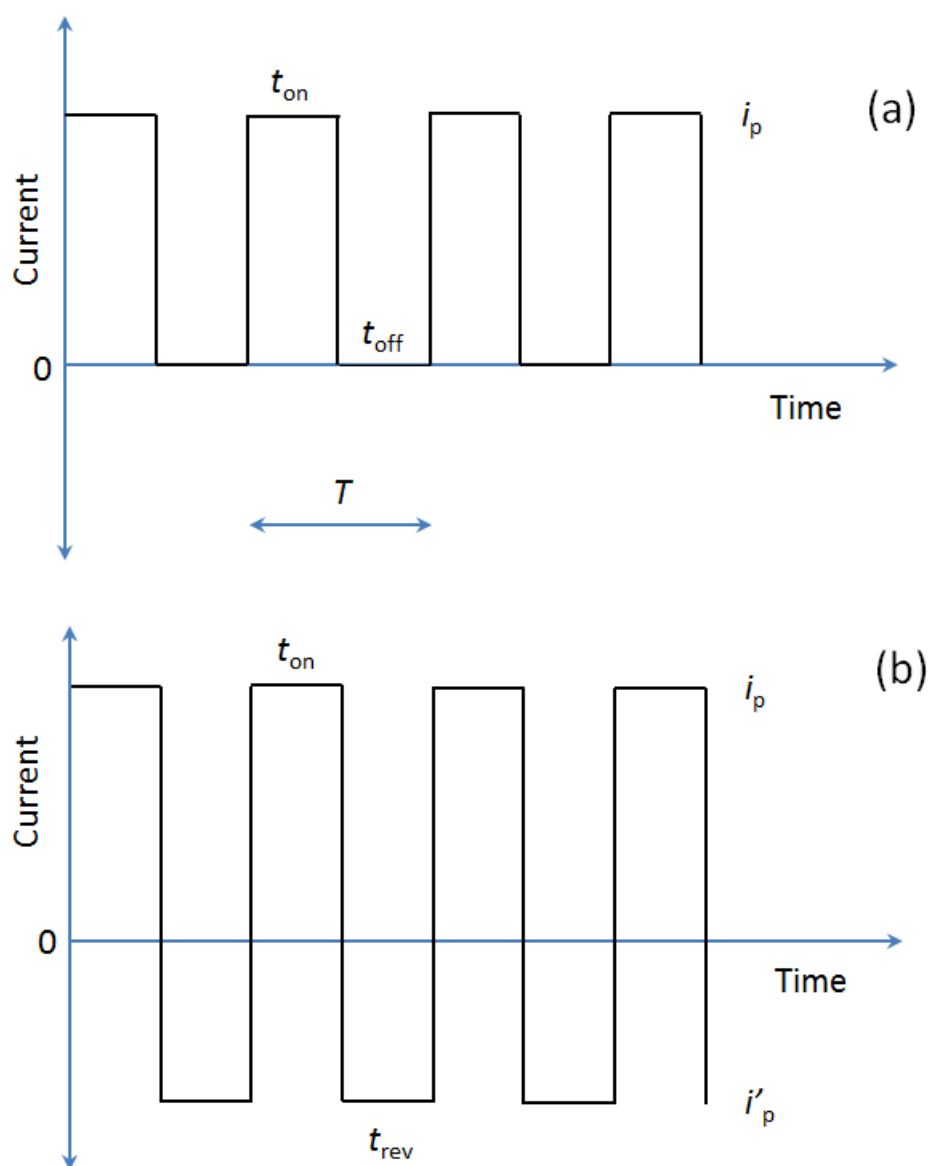


Fig. 1: Pulse current waveforms and definitions for: (a) normal pulse plating and (b) pulse reverse plating.

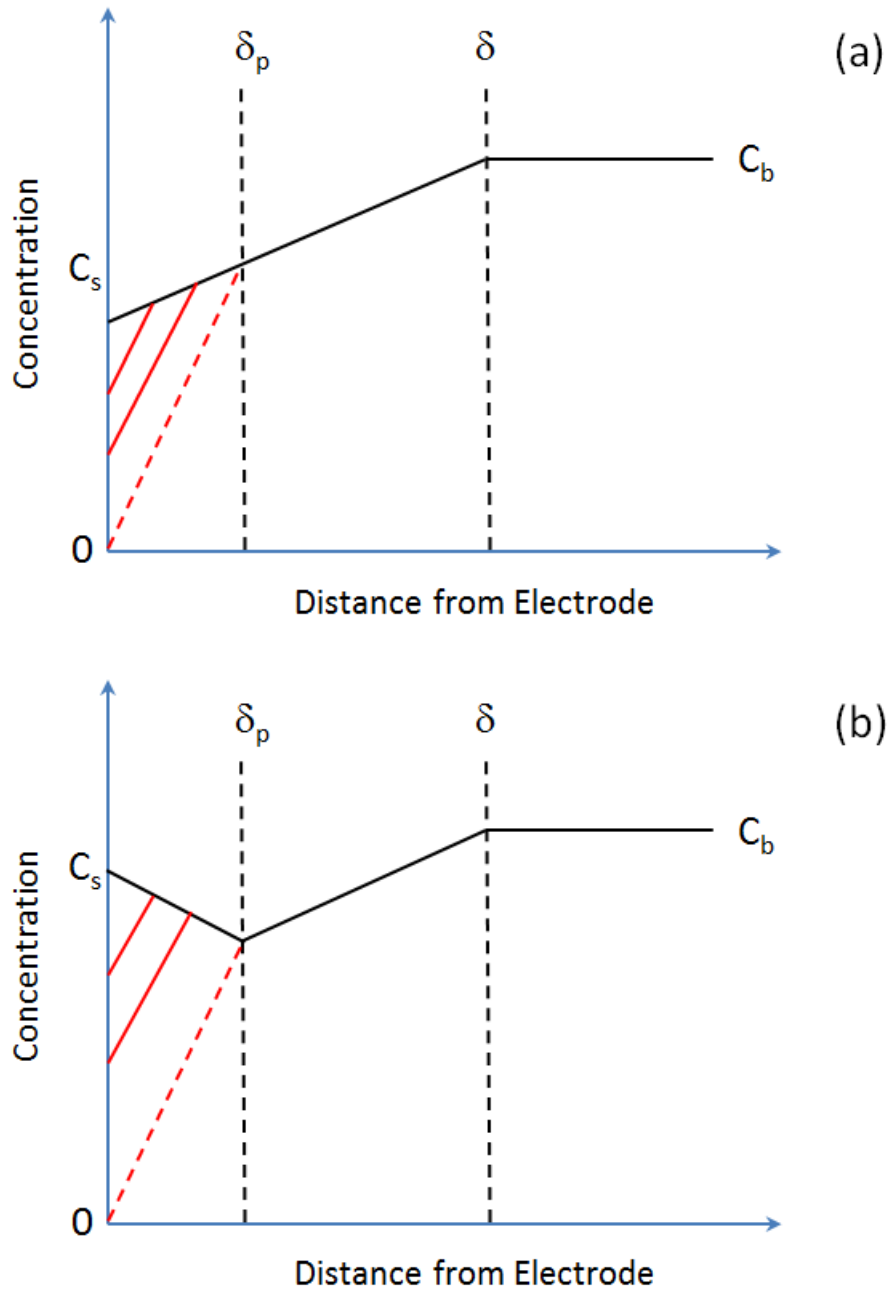


Fig. 2: Schematic diagram of dual diffusion layer formed near the electrode surface according to Ibl⁸ and Yin.¹³ (a) normal pulse plating⁸ (b) pulse reverse plating.¹³ The black lines represent the concentration profile just at the start of the cathodic pulse. Solid red lines show the evolution of the concentration gradient during the pulse. Dotted red line corresponds to the attainment of the pulse limiting current.

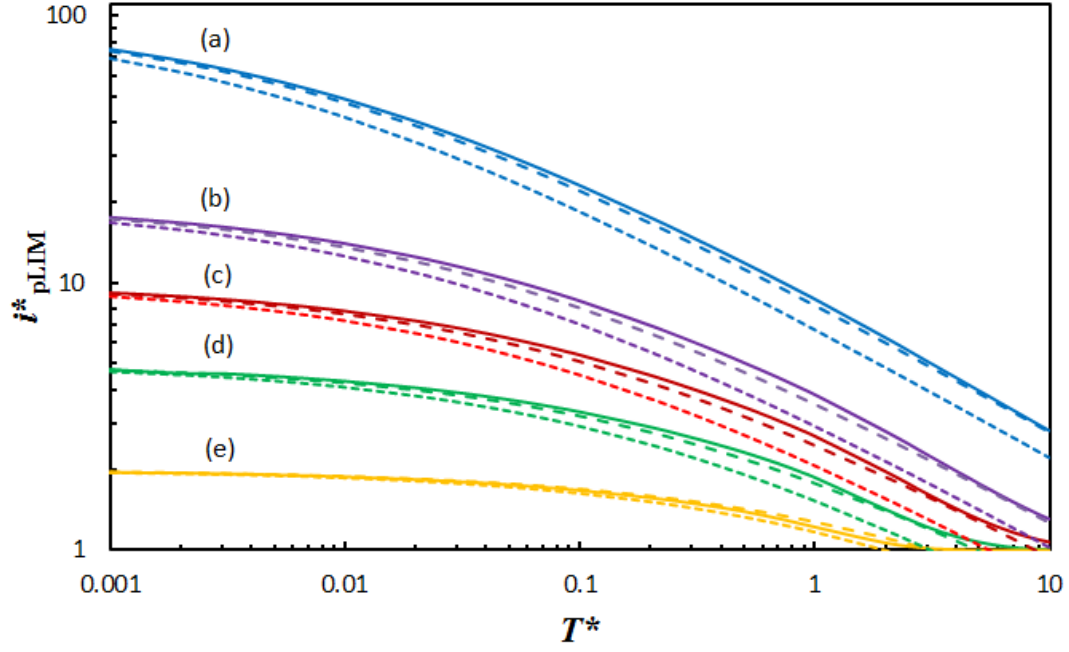


Fig. 3: Plot of the dimensionless pulse limiting current versus the dimensionless pulse time for unipolar pulses at various duty cycles (a) $\theta = 0.01$ (b) $\theta = 0.05$ (c) $\theta = 0.10$ (d) $\theta = 0.20$ (e) $\theta = 0.50$. The solid lines represent equation 5. Long dashed lines are plots of equation 6 with $\alpha = \sqrt{4/\pi}$; short dashed lines are plots of equation 6 with $\alpha = \sqrt{2}$.

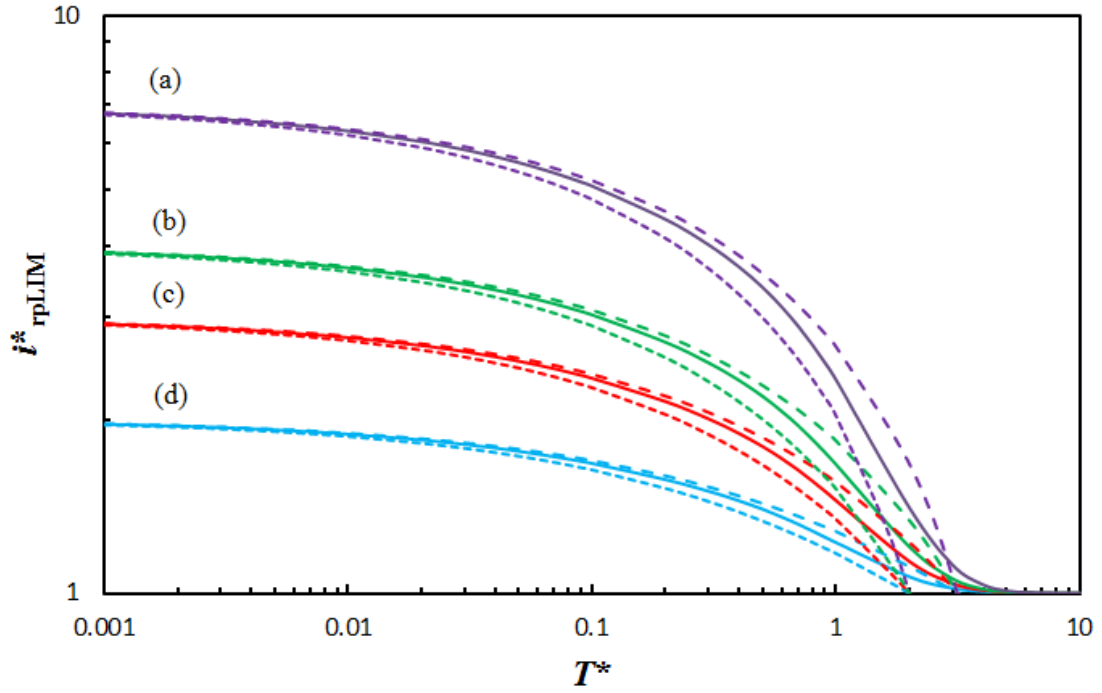


Fig. 4: Plot of the dimensionless pulse reverse limiting current versus the dimensionless pulse time for bipolar and unipolar pulses at a fixed duty cycle of $\theta = 0.50$ and at various values of the pulse reverse limiting current (a) $i^{*} = 5$ (b) $i^{*} = 2$ (c) $i^{*} = 1$ (d) $i^{*} = 0$. The solid lines represent equation 5. Long dashed lines are values derived from equation 4 and with δ_p defined by equation 3. Short dashed lines are calculated from equation 4 and with δ_p defined by equation 2.

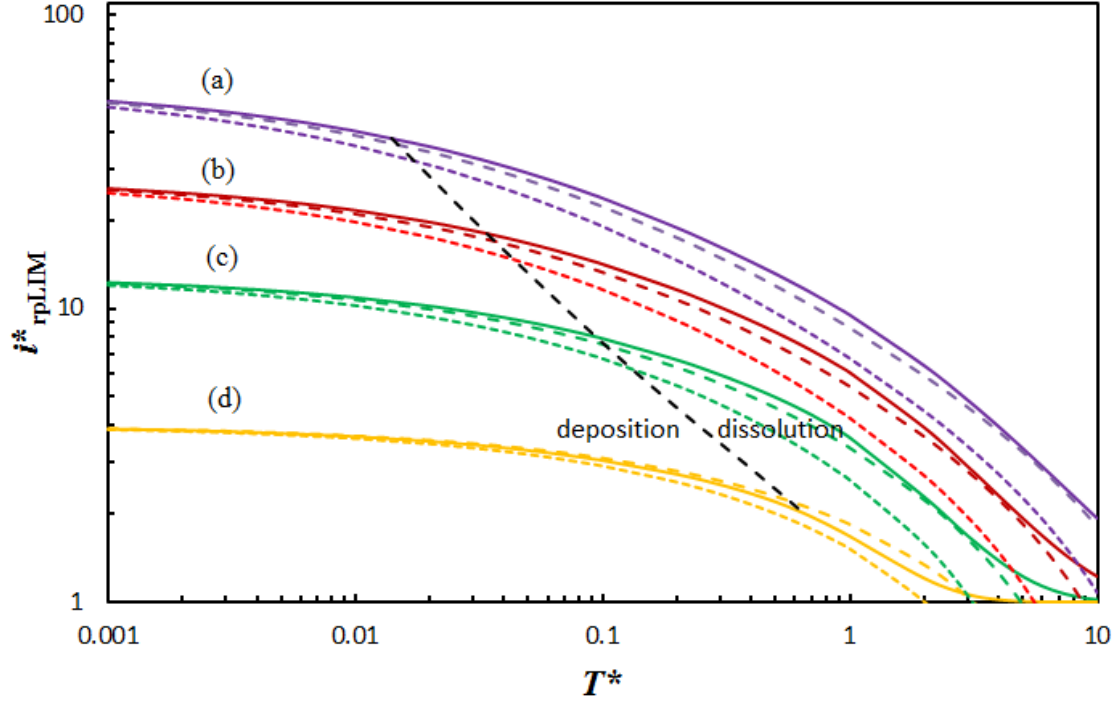


Fig. 5: Plot of the dimensionless pulse reverse limiting current versus the dimensionless pulse time for bipolar pulses with $i^* = 2$ at various duty cycles (a) $\theta = 0.05$ (b) $\theta = 0.10$ (c) $\theta = 0.20$ (d) $\theta = 0.50$. The solid lines represent equation 5. The long dashed lines are values derived from equation 4 and with δ_p defined by equation 3. Short dashed lines are calculated from equation 4 with δ_p defined by equation 2.